

An Insight into Alkali Promotion: A Density Functional Theory Study of CO Dissociation on K/Rh(111)

Zhi-Pan Liu and P. Hu*

Contribution from the School of Chemistry, The Queen's University of Belfast, Belfast BT9 5AG, U.K.

Received June 12, 2001. Revised Manuscript Received August 29, 2001

Abstract: The important role of alkali additives in heterogeneous catalysis is, to a large extent, related to the high promotion effect they have on many fundamental reactions. The wide application of alkali additives in industry does not, however, reflect a thorough understanding of the mechanism of their promotional abilities. To investigate the physical origin of the alkali promotion effect, we have studied CO dissociation on clean Rh(111) and K-covered Rh(111) surfaces using density functional theory. By varying the position of potassium atoms relative to a dissociating CO, we have mapped out the importance of different K effects on the CO dissociation reactions. The K-induced changes in the reaction pathways and reaction barriers have been determined; in particular, a large reduction of the CO dissociation barrier has been identified. A thorough analysis of this promotion effect allows us to rationalize both the electronic and the geometrical factors that govern alkali promotion effect: (i) The extent of barrier reductions depends strongly on how close K is to the dissociating CO. (ii) Direct K–O bonding that is in a very short range plays a crucial role in reducing the barrier. (iii) K can have a rather long-range effect on the TS structure, which could reduce slightly the barriers.

1. Introduction

Alkali effects in heterogeneous catalysis have been a hot topic in the past few decades^{1–15} because alkali additives, e.g., potassium, can greatly enhance the rate of many important catalytic reactions, such as ammonia synthesis^{1,2} and Fischer–Tropsch reactions.^{3,4} Due to the difficulty in directly observing microscopic processes of reactions, most theoretical and experimental studies to date have focused on coadsorption systems involving alkali atoms^{6,7} (especially CO + K systems). These studies have provided some insight into the alkali–adsorbate interaction at the initial state (IS) or the final state (FS) of reactions. On the basis of the understanding gleaned from alkali–adsorbate coadsorption systems, explanations for the

alkali effect on catalytic reactions have been suggested, despite a lack of information on the reaction intermediates and reaction pathways. Some recent theoretical work takes one step beyond the coadsorption studies. Using density functional theory (DFT), Norskov and co-workers reported the reaction pathways of alkali-promoted N₂ dissociation,⁸ and Wilke and Cohen studied the alkali-poisoned H₂ dissociation⁹ in detail. In particular, a classical electrostatic interaction model has been suggested by Norskov and co-workers, which indicated that the electrostatic interaction plays an important role in the alkali promotion effect. However, there are two crucial questions remaining to be answered in this field: (i) How are the reaction pathway and the reaction barrier modified by the alkali? (ii) What is the origin of such modifications? Aiming at answering these questions, we report in this paper an extensive DFT study on the mechanism of K-promoted CO dissociation on Rh(111).

To date, three types of alkali–adsorbate interactions have been proposed to explain the alkali effect: (1) *Direct orbital overlap* between the adsorbate and the alkali metal atom.^{7,10} The range of this interaction is very short, ca. 3 Å. (2) *Interaction of the alkali-induced electric field with adsorbate–surface bonding.*¹¹ This *electrostatic interaction* is typically about 4 Å. (3) The *indirect interaction* mediated by surface electrons.¹² This can be a long-range effect (>4 Å). Experimental evidence, however, indicates that the promotion effect of alkali metal, e.g., potassium, on metal surfaces is predominantly a local one (short-range),^{13–15} and the alkali-induced long-range effect is believed to be less important. Of the two shorter-range interactions, the electrostatic interaction has received much more attention since the 1980s.¹¹

The electrostatic interaction model originates from the highly ionic bonding nature of alkali adsorption, which involves a considerable amount of electron donating and accepting.¹⁶ To lowest order this electrostatic interaction can be considered as

* Corresponding author. E-mail: P.Hu@qub.ac.uk.

(1) Tennison, S. R. In *Catalytic Ammonia Synthesis*; Jennings, J. R., Ed.; Plenum: New York, 1991; p 303.

(2) Hinrichsen, O.; Rosowski, F.; Mulhler, M.; Ertl, G. *Chem. Eng. Sci.* **1996**, *51*, 1683.

(3) Kiskinova, M. P. *Poisoning and Promotion in Catalysis Based on Surface Science Concepts and Experiments*; Studies in Surface Science and Catalysis 70; Elsevier: Amsterdam, 1992.

(4) Somorjai, G. A. *Introduction to surface Chemistry and Catalysis*; Wiley: New York, 1994; p 442.

(5) Hammer, B.; Norskov, J. K. *Adv. Catal.* **2000**, *45*, 71.

(6) Bonzel, H. P.; Pirug, G. In *The Chemical Physics of Solid Surfaces*; King D. A., Woodruff, D. P., Eds.; Elsevier: Amsterdam, 1993; Vol. 6, p 51.

(7) Toomes, R. L.; King, D. A. *Surf. Sci.* **1996**, *349*, 19.

(8) Mortensen, J. J.; Hammer, B.; Norskov, J. K. *Phys. Rev. Lett.* **1998**, *80*, 4335.

(9) Wilke, S.; Cohen, M. H. *Surf. Sci.* **1997**, *380*, 1446.

(10) Solymosi, F.; Berko, A.; Toth, Z. *Surf. Sci.* **1993**, *285*, 197.

(11) Lang, N. D.; Holloway, S.; Norskov, J. K. *Surf. Sci.* **1985**, *150*, 24. Norskov, J. K.; Holloway, S.; Lang, N. D. *Surf. Sci.* **1984**, *137*, 65. Norskov, J. K.; Holloway, S.; Lang, N. D. *J. Vac. Sci. Technol. A* **1985**, *3* (3), 1668.

(12) Feibelman, P. J.; Hamann, D. R. *Phys. Rev. Lett.* **1984**, *52*, 61.

(13) Wandelt, K. In *Physics and Chemistry of Alkali Metal Adsorption*; Bonzel, H. P., Bradshaw, A. M., Ertl, G., Eds.; Elsevier: Amsterdam, 1989; p 25.

(14) Crowell, J. E.; Somorjai, G. A. *Appl. Surf. Sci.* **1984**, *19*, 73.

(15) Pirug, G.; Bonzel, P. *Surf. Sci.* **1988**, *199*, 371.

(16) Gurney, R. W. *Phys. Rev.* **1935**, *47*, 479.

a dipole–dipole interaction. Norskov et al.¹¹ calculated a single K atom adsorption on a semi-infinite jellium surface. They showed that the electrostatic potential is lowered at the adsorption sites directly adjacent to the K atom. It was suggested that the lowered potential would stabilize electronegative adsorbates through dipole–dipole interactions and induce charge transfer from the surface to the antibonding state of electronegative adsorbates, which facilitates the dissociation of the adsorbates (like CO and N₂). Mortensen et al.⁸ calculated alkali-promoted N₂ dissociation on Ru(0001), and the dipole–dipole interaction model was used to interpret their results. Their results show a 0.1–0.2 eV barrier reduction for reactions on Na-promoted Ru, and up to 0.3 eV if Cs is used (the reaction barrier for N₂ dissociation on clean Ru(0001) was reported to be 1.36 eV¹⁷). Janssens et al.¹⁸ measured the surface potential of K-covered Rh(111) experimentally. They showed that the potential close to a K atom (<4 Å) decreases in the order of 1–2 eV and the potential about 4 Å away from the K atom is nearly constant but 0.4–1.0 eV lower than that on clean Rh(111). Janssens et al. suggested that the measured potential reduction could be approximated as an effect of the simple dipole interaction.

An obvious conclusion from the electrostatic model that is supported by some experimental and theoretical work¹⁹ is that electropositive adsorbate (e.g., alkali metals) will promote reactions involving electronegative adsorbates but poison reactions involving electropositive adsorbates, and vice versa. However, this simple model does not sit comfortably with *all* experimental observations, some of which are summarized as follows.

(1) Alkali metals poison reactions involving electronegative adsorbates. It was found experimentally that alkali metals can poison H₂ dissociation on a series transition metal surfaces.^{9,20–22} Consistent with these experiments, DFT calculations for H₂ dissociation on Pd(100) and K-covered Pd(100) by Wilke and Cohen⁹ showed that the K atom retarded H₂ dissociation, despite promoting H atom adsorption.

(2) The isotope exchange has been observed for CO adsorption with high K coverages on Ru(0001),²³ Ni(111),²⁴ Rh(111),²⁵ and Co(10 $\bar{1}0$)⁷ surfaces. It is difficult to apply the electrostatic model to explain such a phenomenon. An alternative model was proposed by Bonzel,²⁶ who suggested that a transient O–K bond could help exchange O between adsorbed CO. There is much experimental work in support of this mechanism. In addition, the structure determination for K + CO coadsorption on Co(10 $\bar{1}0$) by Toomes and King⁷ also favors such a direct K–O interaction mechanism.

It is clear, therefore, that a coherent mechanism for the alkali promotion effect has not yet been established.⁹ With the aim of shedding light on the alkali promotion effect, we have carried out DFT calculations to examine the alkali-induced CO dis-

sociation on Rh(111). We will show in this paper how different kinds of interactions, both the electrostatic interaction and the direct orbital overlap, contribute to the alkali promotion of CO dissociation on Rh(111). With the help of the DFT calculations as a “computational experiment”, we have mapped out the relative importance of the different interactions to the CO dissociation reaction barrier. By examining CO dissociation at different CO–K distances, we have found that it is direct CO–K bonding that enhances greatly the efficiency of CO dissociation on Rh(111). Although this paper focuses on CO dissociation on Rh(111), it is concerned with the basic mechanism involved in the alkali effect on transition metal catalysts. In addition, the origin of the poisoning effect in heterogeneous catalysis is discussed. Therefore, it should be of general interest.

The remainder of the paper is outlined as follows. Our calculation methods are described in section 2. In section 3, we first compare the adsorption of K and O on Rh(111), and then we examine the K effect on O and C adsorption in the K + O/Rh(111) and the K + C/Rh(111) coadsorption systems. At the end of section 3, we show our calculation results for the K-promoted CO dissociation. In section 4, we focus on the interaction between K and the C–O transition-state complex. The effect of this interaction on the reaction barrier is analyzed and discussed in detail. Our conclusions are summarized in section 5.

2. Methods

Density functional theory (DFT) calculations²⁷ with the generalized gradient approximation²⁸ were performed. The electronic wave functions were expanded in a plane wave basis set, and the ionic cores were described by ultrasoft pseudopotentials.²⁹ For the K pseudopotentials, it had been found that the explicit inclusion of semicore states (3s 3p) as valence states was essential. In this work the Rh(111) surface was modeled by a large unit cell, p(3 × 3), with three layers, which were fixed at their bulk-truncated positions. The large unit cell was required to avoid direct interaction between adsorbates in adjacent unit cells and, in the meantime, minimize the bonding competition between all the adsorbates. The surface relaxation was checked, and its effect on the reaction barrier concerned was found to be rather small (within 0.1 eV). The vacuum region between slabs was 10 Å, and a cutoff energy of 340 eV was used. The surface Brillouin zone was sampled by 2 × 2 × 1 *k* points, and the convergence was checked by increasing *k* point sampling to 3 × 3 × 1. The difference between 2 × 2 × 1 and 3 × 3 × 1 *k* point sampling was found to be small (0.05 eV). Previous work also shows that this setup affords sufficient accuracy^{30–33} for investigating reaction pathways and reaction energy profiles. The K-covered Rh(111) surface is modeled by adding one K atom on a hcp hollow site (the most stable site calculated, which is consistent with experiment¹⁸) in a p(3 × 3) unit cell (1/9 ML (monolayer)). The equilibrium height of K on Rh(111) was calculated to be 2.88 Å.

Transition states (TSs) of reactions were searched using a constrained minimization technique.^{32–34} The TS was identified when (i) the force on the atoms vanishes and (ii) the energy is a maximum along the reaction coordinate but a minimum with respect to all remaining degrees of freedom.

3. Results

To investigate the promotion effect of K on CO dissociation, we first examined the bonding nature of K/Rh(111) and O/Rh-

(17) Mortensen, J. J.; Morikawa, Y.; Hammer, B.; Norskov, J. K. *J. Catal.* **1997**, *169*, 85.

(18) Janssens, T. V. W.; Castro, G. R.; Wandelt, K.; Niemantsverdriet, J. W. *Phys. Rev. B* **1994**, *49*, 14599.

(19) Wimmer, E.; Fu, C. L.; Freeman, A. J. *Phys. Rev. Lett.* **1985**, *55*, 2628.

(20) Ertl, G.; Lee, S. B.; Weiss, M. *Surf. Sci.* **1981**, *111*, L711.

(21) Brown, J. K.; Luntz, A. C.; Schultz, P. A. *J. Chem. Phys.* **1991**, *95*, 3767.

(22) Zhou, X. L.; White, J. M. *Surf. Sci.* **1987**, *185*, 450.

(23) Depaola, R. A.; Hrbek, J.; Hoffmann, F. M. *J. Chem. Phys.* **1985**, *82*, 2484.

(24) Lee, J.; Arias, J.; Hanrahan, C. P.; Martin, R. M.; Metiu, H. *Phys. Rev. Lett.* **1983**, *51*, 1991.

(25) Crowell, J. E.; Tysøe, W. T.; Somorjai, G. A. *J. Phys. Chem.* **1985**, *89*, 1598.

(26) Bonzel, H. P. *Surf. Sci. Rep.* **1988**, *8*, 2.

(27) Payne, M. C.; Teter, M. P.; Allan, D. C.; Arias, T. A.; Joannopoulos, J. D.; *Rev. Mod. Phys.* **1992**, *64*, 1045.

(28) Perdew, J. P.; Chevary, J. A.; Vosko, S. H.; Jackson, K. A.; Pederson, M. R.; Singh, D. J.; Fiolhais, C. *Phys. Rev. B* **1992**, *46*, 6671.

(29) Vanderbilt, D. *Phys. Rev. B* **1990**, *41*, 7892.

(30) Liu, Z.-P.; Hu, P.; Alavi, A. *J. Chem. Phys.* **2001**, *114*, 5956.

(31) Liu, Z.-P.; Hu, P. *J. Chem. Phys.* **2001**, *114*, 8244.

(32) Zhang, C. J.; Hu, P. *J. Am. Chem. Soc.* **2000**, *122*, 2134.

(33) Zhang, C. J.; Hu, P.; Alavi, A. *J. Am. Chem. Soc.* **1999**, *121*, 7931.

(34) Alavi, A.; Hu, P.; Deutsch, T.; Silverstrelli, P. L.; Hutter, J. *Phys. Rev. Lett.* **1998**, *80*, 3650.

Table 1. Energetics and Structures of O and C Adsorption on Clean and K-Covered Rh(111)^a

| | O (fcc) | O in O + K | |
|-----------------------------|--------------------|-------------|------------------|
| | | nearest-fcc | next-nearest-fcc |
| E_{ad} (eV) | 4.78 | 4.92 | 4.83 |
| $d_{\text{O-Rh}}$ (Å) | 2.032 ^b | 2.061 | 2.043 |
| ΔE_{ad} (eV) | 0 | +0.14 | +0.05 |
| $d_{\text{O-K}}$ (Å) | | 3.366 | 4.445 |
| | C (hcp) | C in C + K | |
| | | nearest-hcp | next-nearest-hcp |
| E_{ad} (eV) | 7.12 | 7.25 | 7.13 |
| $d_{\text{C-Rh}}$ (Å) | 1.909 | 1.917 | 1.911 |
| ΔE_{ad} (eV) | 0 | +0.13 | +0.01 |
| $d_{\text{C-K}}$ (Å) | | 3.211 | 5.023 |

^a E_{ad} is the O or C chemisorption energy with respect to the free atom, and ΔE_{ad} is the O or C chemisorption energy change in the presence of K. ^b Exp: 2.00 ± 0.08 Å for $c(2 \times 2)$ -O phase.

(111). The direct comparison between these two systems proved to be very enlightening. Following this, we examined the K–O and K–C interaction at the K + O/Rh(111) and K + C/Rh(111) coadsorption systems. At the end of this section, the calculation results for CO dissociation on clean and K-covered Rh(111) are presented.

3.1. Comparison between O/Rh(111) and K/Rh(111).

Atomic chemisorption on transition metal surfaces has been extensively studied over the past few decades.^{35–37} On the basis of the Anderson–Grimley–Newns model,³⁵ Hammer and Norskov³⁶ have suggested that atomic (e.g., C, O) adsorption is achieved via two steps: First, the valence states of the adatom interact with the surface s (p) band, which is fairly wide. This broadens the adatom valence states, forming a single resonance. Second, this resonance will further covalently interact with the surface d band. This model has been successfully applied to the adsorption of some simple electronegative atoms, like H and O.³⁷ In contrast, for the alkali metal, e.g., K, adsorption on transition metal surfaces has long been a controversial issue. Different groups have suggested different bonding models, such as ionic bonding³⁸ and covalent bonding³⁹ as well as combined ionic and metallic bonding.⁴⁰ The recent experimental and theoretical work by King and co-workers⁴⁰ seemed to finally elucidate this issue: K adsorption on metal surfaces was found to possess both ionic and metallic bonding properties, but no covalent bonding character. Here we compare the bonding in O/Rh(111) with that in K/Rh(111) in order to provide some clue for the K–adsorbate interaction in the CO dissociation.

The adsorption energy and the preferred adsorption sites for C and O atoms on Rh(111) (1/9 ML) were first calculated. The adsorption energies and the bond lengths are listed in Table 1. We found that C prefers the hcp hollow site on Rh(111) with a high chemisorption energy (7.12 eV, relative to the free C atom), while O favors the fcc hollow site over the hcp hollow site slightly by about 0.1 eV, which is consistent with the experiment⁴¹ and the previous DFT work.^{42,43} The determined Rh–O bond length (2.032 Å) agrees well with the experimental data (2.00 ± 0.08 Å in $c(2 \times 2)$ -O phase⁴¹). The calculation

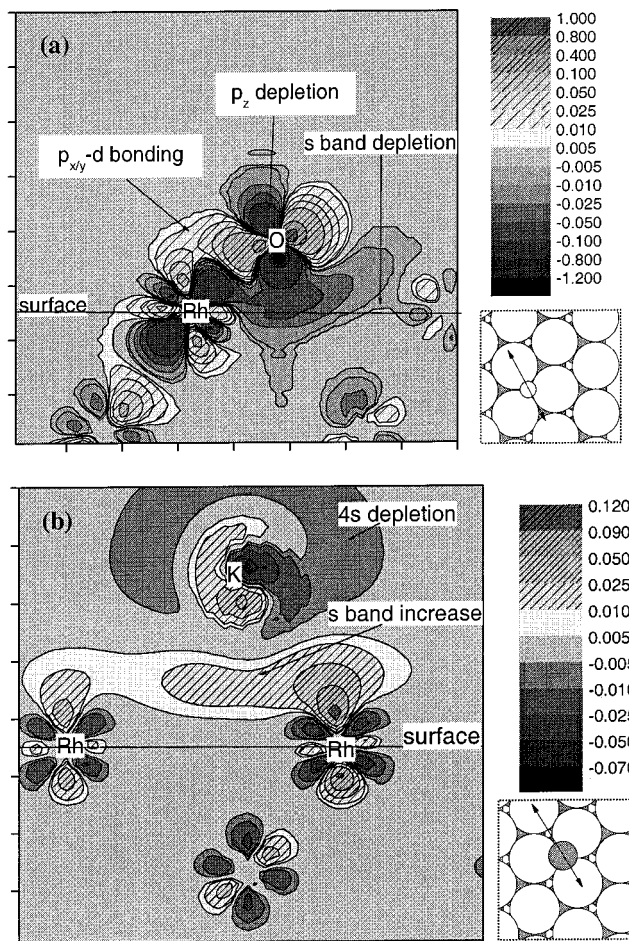


Figure 1. Charge density difference plots for single-atom adsorption of (a) K/Rh(111) and (b) O/Rh(111). The cutting plane is shown in the lower right corner of each figure. All the planes are normal to the Rh (big circle) surface and across the center of the investigated atom (O, small white circle in (a); or K, middle gray circle in (b)). The unit of charge density is $e/\text{Å}^3$. The unit of both axes is Å.

reported by Walter, Lewis, and Rappe⁴² also shows a very small fcc–hcp energy difference (0.11 eV) for the O adsorption (0.25 ML) on the Rh(111) surface.

To compare K and O adsorption on Rh(111), we have calculated the total charge density difference,^{44,45} $\Delta\rho(\mathbf{r})$, for O/Rh(111) (Figure 1a) and K/Rh(111) (Figure 1b). The $\Delta\rho(\mathbf{r})$ for the X/Rh(111) (X = O or K) systems were constructed as follows:

$$\Delta\rho(\mathbf{r}) = r_{\text{X/Rh(111)}}(\mathbf{r}) - \rho_{\text{X}}(\mathbf{r}) - \rho_{\text{Rh(111)}}(\mathbf{r}) \quad (1)$$

where $r_{\text{X/Rh(111)}}(\mathbf{r})$ is the total charge density distribution of the X/Rh(111) system; $\rho_{\text{X}}(\mathbf{r})$ and $\rho_{\text{Rh(111)}}(\mathbf{r})$ are the total charge density distributions of the isolated X adlayer and Rh(111), respectively. The calculations for the isolated systems were in supercells and under conditions identical to those employed for the X/Rh(111) systems. Furthermore, the atomic positions for

(35) Anderson, P. W. *Phys. Rev.* **1961**, *124*, 41. Grimley, T. B. *Proc. Phys. Soc. London Sect. A* **1967**, *90*, 751. Newns, D. M. *Phys. Rev.* **1969**, *178*, 1123.

(36) Hammer, B.; Norskov, J. K. *Surf. Sci.* **1995**, *343*, 211. Hammer, B.; Norskov, J. K. *Nature* **1995**, *376*, 238.

(37) Brivio, G. P.; Trioni, M. I. *Rev. Mod. Phys.* **1999**, *71*, 231.

(38) Langmuir, I. *J. Am. Chem. Soc.* **1932**, *54*, 2798.

(39) Ishida, H. *Surf. Sci.* **1991**, *242*, 341.

(40) Jenkins, S. J.; King, D. A. *Chem. Phys. Lett.* **1999**, *309*, 434.

(41) Schwegmann, S.; Over, H.; De Renzi, V.; Ertl, G. *Surf. Sci.* **1997**, *375*, 91.

(42) Walter, E. J.; Lewis, S. P.; Rappe, A. M. *J. Chem. Phys.* **2000**, *113*, 4338.

(43) Ganduglia-Pirovano, M. V.; Scheffler, M. *Phys. Rev. B* **1999**, *59*, 15533.

(44) Bader, R. F. *Atoms in Molecules: A Quantum Theory*; Oxford University Press: Oxford, 1990.

(45) Jenkins, S. J.; King, D. A. *Chem. Phys. Lett.* **2000**, *317*, 372.

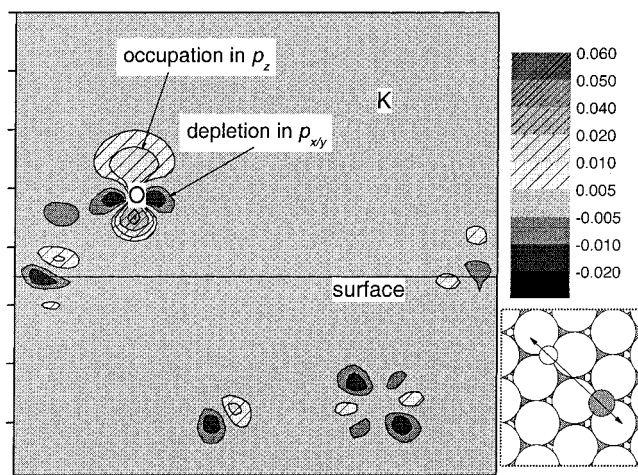


Figure 2. Charge density difference plots for K + O/Rh(111). The O atom is at the next-nearest-fcc site with respect to the K atom. The cutting plane is shown in the lower right corner (the description of it is similar to that in the Figure 1 caption). The unit of charge density is $e/\text{\AA}^3$. The unit of both axes is \AA .

both isolated systems were precisely those determined from the X/Rh(111) systems.

Figure 1a reveals a strong p–d bonding character in O/Rh(111): Strong *mixing* between the O $2p_x(p_y)$ and Rh “d-like” orbital forms a *covalent bond* between O and Rh. At the same time, the charge densities in the O $2p_z$ and Rh d_{z^2} -like orbitals are strongly depleted. This is, however, mainly in the core regions. Outside the two direct bonding atoms (the O and the Rh labeled), the electrons beneath the O atom, which are in a fairly delocalized shape, are driven away, which appears to be due to a depletion in the surface s electrons. This is consistent with the model described by Harris and Andersson for H_2 dissociation on a metal surface,⁴⁶ which addressed the repulsion between the adsorbate and the surface s electrons. In essence, the O adsorption on Rh(111) can be described as follows: (i) the metal s electrons near the O atom are considerably depleted; (ii) the O $2p_x$ ($2p_y$) plays a positive role in the O/Rh bond formation; and (iii) the O $2p_z$ is depleted, which is due to the Pauli repulsion.

In contrast to the bonding of O on Rh(111), Figure 1b shows that for K adsorption the charge density outside the K core (4s electrons, about 2\AA from the center of K) is depleted, while there are delocalized electrons accumulated near the surface, forming “an extra layer”. It is apparent that the K atom donates electrons substantially to Rh(111) (also see section 4). The rather localized metal d electrons also appear to slightly reorient, especially for the Rh atoms directly adjacent to the K atom: The charge density in the Rh d_{z^2} -like orbital increases, while the charge density is depleted in the d_{xz} -like orbital. This d orbital rearrangement is just opposite to that in the case of O adsorption (see Figure 1a). Near the core of the K atom, it is found that the charge density (which mainly belongs to the 3s and 3p states) is polarized toward the surface. Compared to the O/Rh bonding in Figure 1a, the K/Rh bonding is more ionic and metallic than covalent, with the dominant feature of K adsorption being the K 4s electron delocalization into the surface. The K/Rh bonding picture described here is essentially the same as the previous work on K/Co(1010) by Jenkins and King⁴⁰ and on the Cs/W(001) system by Wimmer et al.⁴⁷

3.2. Interaction in the Coadsorption Systems: K + O/Rh(111) and K + C/Rh(111). Due to the presence of K, the bonding of C and O with Rh(111) will be modified. We have investigated the K influence on the C or the O adsorption by varying the distance between the K and the C or the O atoms. For O, two configurations, O on the nearest-fcc and next-nearest-fcc sites with respect to the K, were studied. Similarly, for C, C at the nearest-hcp and next-nearest-hcp sites with respect to K were calculated. The K-induced chemisorption energy changes (ΔE_{ad}) together with the optimized adsorption structures are listed in Table 1. It shows that generally the chemisorption energy of C or O increases ($\Delta E_{\text{ad}} > 0$) in the presence of the K atom. When O is on the next-nearest-fcc site, such stabilization is rather weak (0.05 eV), while on the closer site (the nearest-fcc site) the chemisorption energy of O is increased by 0.14 eV. The same trend is also observed for C. It appears that the closer C or O is to the K, the higher the chemisorption energy of C or O will be. As for the adsorption structure, interestingly, both the C–Rh and O–Rh bond lengths increase in the presence of K. This implies a bond weakening between C (O) and the surface (this will be further discussed below).

In the following subsections, all the charge density differences, $\Delta\rho(\mathbf{r})$, for a K + X/Rh(111) system (X = C, O), are constructed as follows:

$$\Delta\rho(\mathbf{r}) = \rho_{\text{K+X/Rh(111)}}(\mathbf{r}) - \rho_{\text{K/Rh(111)}}(\mathbf{r}) - \rho_{\text{X/Rh(111)}}(\mathbf{r}) + \rho_{\text{Rh(111)}}(\mathbf{r}) \quad (2)$$

As with eq 1, the atomic positions for the isolated systems, i.e., K/Rh(111), X/Rh(111), and Rh(111), are identical to those in K + X/Rh(111). The calculated $\Delta\rho(\mathbf{r})$ in eq 2 reflects the charge density redistribution in the coadsorption system compared to that in the single atomic chemisorption system.

3.2.1. K Effect on O Adsorption on the Next-Nearest-fcc Site. Figure 2 is a charge density difference plot for the K + O/Rh(111) coadsorption system with O on the next-nearest-fcc site. It shows that, near the center of the O atom, the charge density in O 2p orbitals is rearranged: The O $2p_z$ -like states are populated, together with a depletion of charge density in the O $2p_x$ ($2p_y$)-like states, which is in contrast to that shown in Figure 1a. It is also obvious that no direct bonding occurs between the K and the O atom, and the charge density redistribution around the K atom is very small (below $\pm 0.005 e/\text{\AA}^3$). This perspective is reasonable, considering that the distance between the K and the O is quite long (4.45\AA). Thus, weak electrostatic interaction between the K and the O dominates. According to the electrostatic interaction model, the negative electric field (directed from O to Rh) induced by the nearby K/Rh will affect the O–Rh bonding by shifting the bonding states to larger binding energies with respect to the E_{F} . This is what we see in the system. From our calculations, for example, the O 2s binding energy shifts down by about 0.1 eV. In particular, the antibonding states with O $2p_z$ character, which are mostly unoccupied without the K, become partially occupied. This picture is consistent with a previous study on CO + K/Ni coadsorption by Wimmer et al.¹⁹ The charge density change around the K being small can also be understood: Since the O/Rh bonding is largely covalent, the O-induced electrostatic field is relatively small, which will have little effect on the K–Rh bonding. It should be emphasized that the K-induced charge transfer into the O–Rh antibonding states should weaken the O–Rh bonding, which is evident from the lengthening of the O–Rh bond (shown in Table 1). However, this O–Rh bond weakening is offset by the electrostatic attraction between K

(46) Harris, J.; Andersson, S. *Phys. Rev. Lett.* **1985**, *55*, 1583.

(47) Wimmer, E.; Freeman, A. J.; Hiskes, J. R.; Kara, A. M. *Phys. Rev. B* **1983**, *28*, 3074.

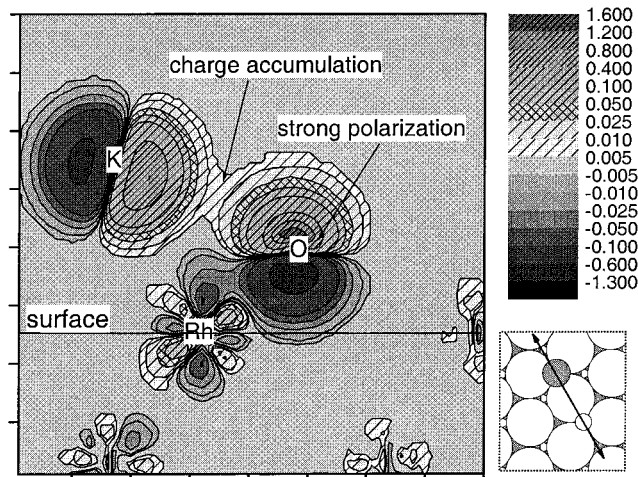


Figure 3. Similar to Figure 2, except that the O atom now is at the nearest-fcc site with respect to the K atom.

(positive) and O (negative), which in total leads to a small increase in the O adsorption energy ($\Delta E_{\text{ad}} = 0.05$ eV).

3.2.2. K Effect on O Adsorption at the Nearest-fcc Site.

When O is at the nearest-fcc site (the K–O distance is 3.37 Å), the interaction between K and O changes considerably, which is displayed in the charge density difference plot in Figure 3. It can be seen from Figure 3 that there is a considerable charge accumulation between K and O, together with strong charge polarization near the core of both the K atom and the O atom. Having compared this K–O interaction picture with that in a free K_2O molecule, we found that the K–O interaction shown in Figure 3 is similar to the ionic bonding between K and O in free K_2O . This indicates that the electrostatic attraction between K and O has evolved into direct bonding when O is at the nearest-fcc hollow site. As a result, this direct K–O interaction has induced a large charge density variation (± 1.30 e/Å³ in Figure 3), in contrast to the relatively small one in Figure 2 (the weak electrostatic interaction). As for the O adsorption structure, the O is found to be farther away from the surface (see the O–Rh distance in Table 1). It should be emphasized that the charge density redistribution induced by the electrostatic interaction shown in Figure 2 is not seen in Figure 3, which implies that the electrostatic interaction is less important at this stage. Despite the weakening of the O–Rh bond, which is reflected in the increased O–Rh distance, the K–O direct bonding largely stabilizes the O atom, resulting in a larger change ($\Delta E_{\text{ad}} = 0.14$ eV) than the electrostatic interaction.

3.2.3. K Effect on C Adsorption. The K effect on the C adsorption is found to be very similar to its effect on the O adsorption (see the energetics and structures in Table 1). However, the calculated ΔE_{ad} values for C are slightly smaller than those for O (Table 1). There may be two reasons for this: First, the C-induced dipole is smaller than that of O, which means that the electrostatic interaction between K and C should be smaller than that between K and O. Second, direct C–K bonding, if it exists, may be weaker than O–K bonding due to the lower electronegativity of C (electronegativity for C = 2.5; O = 3.5; K = 0.8).

From the results above, we can conclude that the long-held electrostatic attraction, which dominates the interaction when the distance between K and a reactant (C or O) is relatively large, only slightly affects the chemisorption energy of the reactant. On the other hand, when K is neighboring with a reactant, the direct bonding between K and the reactant becomes dominant. Such direct bonding appears to be more important

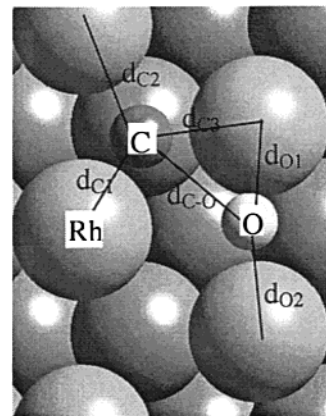


Figure 4. Top view of the TS for CO dissociation on clean Rh(111). The bond lengths used in Table 2 are labeled.

Table 2. TS Structures for CO Dissociation on Clean and K-Covered Rh(111)^a

| | d_{C1} | d_{C2} | d_{C3} | d_{O1} | d_{O2} | $d_{\text{C-O}}$ | $d_{\text{O-K}}$ | $d_{\text{C-K}}$ |
|--------------------|-----------------|-----------------|-----------------|-----------------|-----------------|------------------|------------------|------------------|
| TS ⁰ | 2.029 | 1.890 | 1.959 | 2.046 | 2.145 | 1.865 | | |
| TS(K) ¹ | 2.065 | 1.884 | 1.975 | 2.055 | 2.328 | 1.875 | 2.474 | 3.099 |
| TS(K) ² | 2.010 | 1.890 | 1.988 | 2.038 | 2.406 | 1.943 | 2.791 | 3.269 |
| TS(K) ³ | 2.067 | 1.888 | 1.972 | 2.045 | 2.176 | 1.880 | 4.427 | 3.315 |
| TS(K) ⁴ | 2.055 | 1.888 | 1.965 | 2.055 | 2.245 | 1.890 | 3.674 | 5.012 |

^a The bond lengths, d_{C1} , d_{C2} , d_{C3} , d_{O1} , d_{O2} , and $d_{\text{C-O}}$, in the table are labeled in Figure 4. The unit is Å.

in enhancing reactant chemisorption energies than the electrostatic interaction.

3.3. CO Dissociation on Clean Rh(111) and K-Covered Rh(111).

We first located the transition state of CO dissociation on clean Rh(111) in a $p(3 \times 3)$ unit cell. The TS of this reaction is hereafter named as TS⁰. The reaction barrier is determined to be 1.17 eV with respect to the energy of a gas-phase CO molecule and the clean Rh surface. The TS geometry is depicted in Figure 4, and the structure parameters are listed in Table 2. Three main features for CO dissociation on the clean Rh(111) can be seen from Figure 4. First, in the TS the C is near a hcp hollow site, while the O is close to a bridge site. This TS geometry is consistent with the simple rules suggested by Michaelides and Hu^{48,49} to describe reaction pathways in heterogeneous catalysis: The higher valency adsorbate (e.g., C) occupies the higher coordination site (e.g., 3-fold hcp site) at the TS. Second, the C and the O have to share a surface atom at the TS, which will incur a bonding competition effect^{31,50,51} during the CO dissociation. Such a bonding competition effect^{31,34} is believed to significantly increase the reaction barrier for CO dissociation (see section 4). Third, the C–O distance at the TS⁰ (1.87 Å) is stretched by 65% compared to that of the gas-phase CO (1.13 Å). The long-stretched TS implies that CO dissociation on clean Rh(111) is a late-barrier reaction,^{5,31} which seems to be a common feature as observed for N_2 ^{17,52} and NO ⁵³ dissociation on Ru(0001). For this kind of late-barrier reaction, the TSs look more like the FSs, which means that the properties of the TSs are similar to those of atomic adsorption (FSs) and quite different from those of the ISs in these reactions.^{5,31,53} Therefore, the understanding of the

(48) Michaelides, A.; Hu, P. *J. Am. Chem. Soc.* **2000**, *122*, 9866.

(49) Michaelides, A.; Hu, P. *J. Chem. Phys.* **2001**, *114*, 5792.

(50) Zhang, C. J.; Hu, P. *J. Am. Chem. Soc.* **2001**, *123*, 1166.

(51) Bleakley, K.; Hu, P. *J. Am. Chem. Soc.* **1999**, *121*, 7644.

(52) Dahl, S.; Logadottir, A.; Egeberg, R. C.; Larsen, J. H.; Chorkendorff,

I.; Tornqvist, E.; Norskov, J. K. *Phys. Rev. Lett.* **1999**, *83*, 1814.

(53) Hammer, B. *Surf. Sci.* **2000**, *459*, 323.

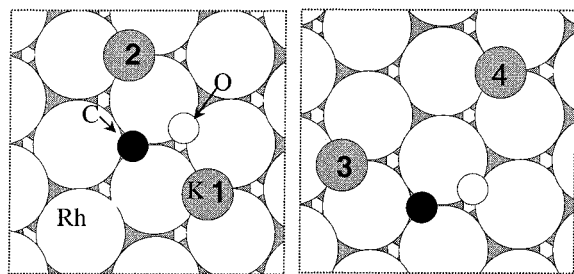


Figure 5. Top view of four TSs of K-promoted CO dissociation on Rh(111). TS(K)¹: C, small black circle; O, small white circle; and K, gray circle number 1. TS(K)², TS(K)³, and TS(K)⁴ are similar to TS(K)¹, except that the K atom is labeled 2, 3, and 4, respectively.

Table 3. Calculated Reaction Barriers (E_a^{dis}) for CO Dissociation on Clean (TS⁰) and K-Covered Rh(111) (TS(K)¹, TS(K)², TS(K)³, and TS(K)⁴)^a

| | TS ⁰ | TS(K) ¹ | TS(K) ² | TS(K) ³ | TS(K) ⁴ |
|----------------------------------|-----------------|--------------------|--------------------|--------------------|--------------------|
| $E_a^{\text{dis}}(\text{fix})$ | 1.17 | 0.72 | 0.84 | 0.93 | 0.98 |
| $E_a^{\text{dis}}(\text{relax})$ | | 0.66 | 0.76 | 0.91 | 0.95 |
| ΔE_a^{dis} | 0 | -0.51 | -0.41 | -0.26 | -0.22 |

^a The K-modified E_a^{dis} values are calculated with (i) *fixed* TS geometry ($E_a^{\text{dis}}(\text{fix})$), in which the C and O atoms are fixed at the same positions as that in the TS⁰ and a new energy is calculated in the presence of K (K is also fixed), and (ii) *relaxed* TS geometry ($E_a^{\text{dis}}(\text{relax})$), in which new TSs in the presence of the K are searched (also see text). The K-induced barrier changes (ΔE_a^{dis}) are also listed. The energy unit is eV.

interaction between K and O (C) introduced in section 3.2 is instructive for understanding the K promotion effect on CO dissociation.

As discussed in section 3.2, when the distance between K and O (or C) is long, the interaction between them is mainly electrostatic, while a direct bonding develops if the distance is short. Considering that electrostatic interaction and direct bonding may have different consequences on CO dissociation, we modeled the K promotion effect on CO dissociation on Rh(111) by placing K at four different positions with respect to the dissociating CO. The TSs corresponding to these four K positions are illustrated in Figure 5, in which the K positions in these TSs are labeled 1–4. When K is at position 1 or 2, defined as TS(K)¹ and TS(K)², respectively, the distance between the dissociating CO complex and the K is quite short, while at position 3 or 4, labeled as TS(K)³ and TS(K)⁴, respectively, the dissociating CO complex is farther away from the K. For these four configurations, we have calculated the K-modified reaction barriers using two structures: (i) the C and O atoms are fixed at the same positions as in the TS⁰ and a new energy is calculated in the presence of K (K is also fixed), and (ii) a new TS in the presence of the K is searched. We found that the reaction barriers determined from these two approaches are similar, within 0.1 eV. The structural parameters of the new TS(K)s are listed in Table 2, together with those of TS⁰. All the reaction barriers are summarized in Table 3.

Compared to the barrier of 1.17 eV for CO dissociation on clean Rh(111), the calculated CO dissociation barriers on the K-covered Rh(111) are reduced. This agrees with the general consensus that K additives promote CO dissociation. More importantly, we found that the barrier reduction is strongly dependent on the K location. The decrease of the calculated reaction barriers at the TS(K)³ and TS(K)⁴ are relatively small, around 0.1–0.2 eV, whereas the reductions of the dissociation barriers are larger at both TS(K)¹ and TS(K)². In particular, at TS(K)¹ the K reduces the CO dissociation barrier by almost half (from 1.17 to 0.66 eV). This means that the reaction rate

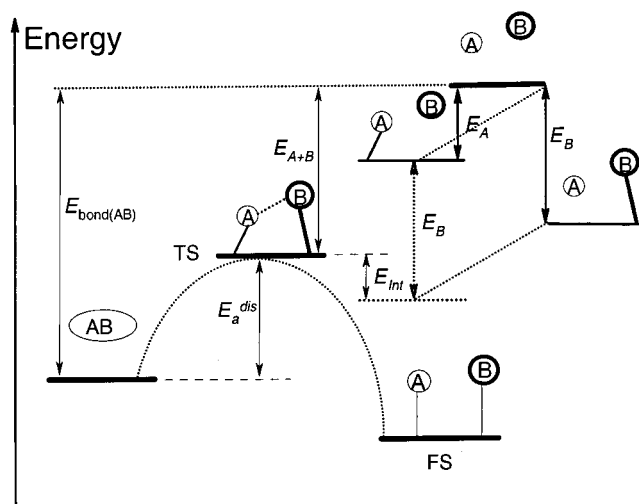


Figure 6. Illustration of an energetic profile of a dissociation reaction, $AB \rightarrow A + B$. The decomposition of total chemisorption energy of A and B (E_{A+B}) at the TS, starting from the A and B atoms in the gas phase, is also shown. All the terms are defined in the text (see eqs 4 and 5).

can be increased by roughly 6 orders of magnitude if the pre-exponential factor is unchanged (assuming $T = 400$ K). Considering the large energy difference between TS(K)¹ and TS(K)⁴, it is expected that in the presence of the K, CO dissociation will largely follow the reaction pathway via TS(K)¹. Thus, the real alkali promotion effects should be mainly associated with the closer configurations, like TS(K)¹ and TS(K)², where the distances between alkali metal atoms and reactants are quite short.

It is of interest to compare our results with those of alkali-promoted N₂ dissociation on Ru(0001) calculated by Mortensen et al.⁸ These two systems are similar: Both involve simple diatomic molecule dissociation on close-packed metal surfaces. The reaction barrier determined for N₂ dissociation on the clean Ru(0001) is 1.36 eV,¹⁷ which is quite similar to 1.17 eV for CO dissociation in our case. Mortensen et al. reported that Na reduces the N₂ dissociation barrier by 0.1–0.2 eV and that of Cs by 0.3 eV. The smaller reduction in barriers due to the presence of alkali metals may seem to be different from our results (the barrier is reduced significantly from 1.17 to 0.66 eV at TS(K)¹ in CO dissociation). In fact, their results are consistent with ours. The position of the alkali atom in their calculations is similar to that of TS(K)³ and TS(K)⁴ in our case: In their calculations, the distances between the alkali metal atoms and reactants are quite long (similar to those in TS(K)³ and TS(K)⁴), and the closer configurations such as TS(K)¹ and TS(K)² were not calculated for N₂ dissociation on Ru(0001).

4. Discussion

To provide insight into the K promotion effect, the physical origin of the dissociation barrier (E_a^{dis}) and the way that E_a^{dis} responds to K addition need to be well understood. Toward this goal, we use the following scheme to decompose E_a^{dis} . Starting from the C and O atoms in the gas phase shown in Figure 6, the dissociation barrier (E_a^{dis}) with respect to the gas-phase CO molecule is written as

$$E_a^{\text{dis}} = E_{\text{bond}(\text{CO})} - E^{\text{TS}} \quad (3)$$

where $E_{\text{bond}(\text{CO})}$ is the CO bonding energy in the gas phase and E^{TS} is the chemisorption energy of C–O complex at the TS

Table 4. Reaction Barrier Decomposition (Eq 5) for TS^o, TS(K)¹, and TS(K)⁴^a

| | E_C^{TS} | E_O^{TS} | $E_{\text{int}}^{\text{TS}}$ | E_a^{dis} |
|--------------------|-------------------|-------------------|------------------------------|--------------------|
| TS ^o | 7.02 | 4.15 | 1.11 | 1.17 |
| TS(K) ¹ | 7.12 | 4.38 | 0.94 | 0.66 |
| TS(K) ⁴ | 7.04 | 4.17 | 0.95 | 0.95 |

^a Each term in the table is defined in the text. The unit is eV.

with respect to the C and O atoms in the gas phase. In this work, the calculated $E_{\text{bond}(\text{CO})}$ (11.23 eV) was used to obtain all the reaction barriers. This value agrees well with the experimental value of 11.11 eV. It is worth noting that eq 3 shows E_a^{dis} being only a function of E^{TS} : In the presence of K atoms, E^{TS} will vary, and so does E_a^{dis} .

E^{TS} can then be further decomposed into three terms (see Figure 6):

$$E^{\text{TS}} = E_C^{\text{TS}} + E_O^{\text{TS}} - E_{\text{int}}^{\text{TS}} \quad (4)$$

where E_C^{TS} is the C chemisorption energy at the TS geometry without the O atom and E_O^{TS} is defined in a similar way. The $E_{\text{int}}^{\text{TS}}$ is a quantitative measure of the interaction between C and O at the TS, which is usually a significant part of reaction barriers (see the discussion below). Thus, by combining eq 4 and eq 3, we arrive at

$$E_a^{\text{dis}} = E_{\text{bond}(\text{CO})} - E^{\text{TS}} = E_{\text{bond}(\text{CO})} - E_C^{\text{TS}} - E_O^{\text{TS}} + E_{\text{int}}^{\text{TS}} \quad (5)$$

Equation 5 suggests that the reaction barrier (E_a^{dis}) consists of three parts: (i) $E_{\text{bond}(\text{CO})}$, the bonding energy of CO in the gas phase; (ii) E_C^{TS} and E_O^{TS} , the individual reactant (C, O) adsorption energies at the TS; and (iii) $E_{\text{int}}^{\text{TS}}$, the interaction energy between C and O at the TS.

It is worth discussing the physical meaning of the interaction energy at the TS, $E_{\text{int}}^{\text{TS}}$. $E_{\text{int}}^{\text{TS}}$ is believed to consist mainly of two parts:^{31,54} (i) the so-called *bonding competition effect*,^{34,51} which is caused by the C and the O sharing bonding with one Rh atom, and (ii) the *direct Pauli repulsion* between the C and O atoms,⁵⁴ which is strongly related to the distance between C and O. Obviously, both the bonding competition effect and the Pauli repulsion are sensitive to the TS structure. In particular, the bonding competition effect can be greatly reduced if the reaction occurs on a corrugated surface, where the C and the O do not need to share bonding with the same surface atoms.³¹ Such barrier reduction at corrugated surfaces has been confirmed by both experimental and theoretical work.^{52,53} The intermolecular interaction, e.g., the bonding and the antibonding between C and O in this case, may also contribute to $E_{\text{int}}^{\text{TS}}$. However, this is likely to be small since, as we mentioned before, CO dissociation on the metal surface belongs to the late TS reaction. The stretched C–O bond at the TS implies that the interaction between C and O at the TS resembles the interaction of two *individual adsorbed atoms* rather than the intermolecular interaction.

Using eq 5, we have decomposed E_a^{dis} for TS^o (CO dissociation on the clean Rh(111)) as well as TS(K)¹ and TS(K)⁴ (reactions on K covered Rh(111)). The results are listed in Table 4. It is shown that, with the addition of K, all the components of the reaction barrier, E_C^{TS} , E_O^{TS} , and $E_{\text{int}}^{\text{TS}}$ are changed: K assists CO dissociation by stabilizing C and O adsorption at the TS (E_C^{TS} , E_O^{TS}) and also by reducing $E_{\text{int}}^{\text{TS}}$.

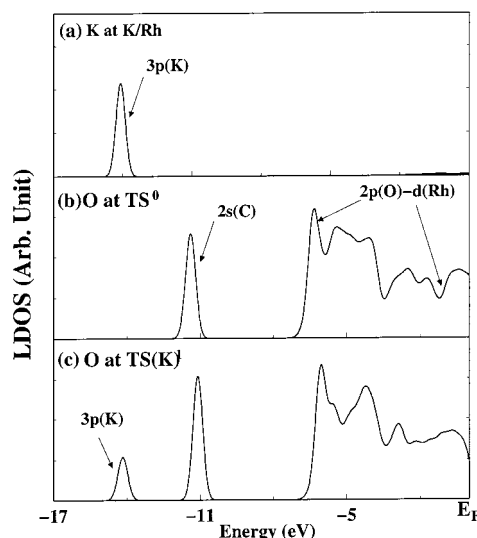


Figure 7. Local density of states (LDOS) projected onto (a) the K atom in K/Rh(111), (b) the O atom at the TS^o, and (c) the O atom at the TS(K)¹.

These two effects together contribute to the reduction of the reaction barrier and will be discussed now in more detail.

4.1. K-Induced O (C) Adsorption Energy Increase at the TSs. From Table 4, E_O^{TS} is increased due to K addition. In particular, at the TS(K)¹, E_O^{TS} increases by 0.23 eV. However, the increase in E_C^{TS} is relatively small (within 0.1 eV). Compared to the C atom, the O atom plays a more important role in interacting with the K atom at the TS. This is consistent with what we have observed in the K + C(O)/Rh(111) coadsorption systems: The K effect on O is more significant than that on C. As mentioned in section 3.2, there is already a direct bonding between K and O when O neighbors the K atom, where the K to O distance is about 3.2–3.4 Å. Therefore, it is expected that at TSs such direct bonding may be further strengthened if the distance between K and the dissociating complex, especially the O atom, is shortened to below 3 Å. Indeed, at TS(K)¹ and TS(K)² the K–O distances are only 2.474 and 2.791 Å, respectively. In contrast, at TS(K)³ and TS(K)⁴ the K–O distances are larger than 3.6 Å. Considering the results discussed in section 3.2 (when the K–O distance is short there is a direct bonding, and if the K–O(C) distance is long the electrostatic interaction dominates), it is expected that a direct K–O bonding has developed at the TS(K)¹ and TS(K)², while the electrostatic interaction plays a role in TS(K)³ and TS(K)⁴. In fact, this explains the calculated energetic results in Table 4: The O atom is strongly stabilized at the TS(K)¹ ($E_O^{\text{TS}} = 4.38$ eV), while such stabilization is smaller at TS(K)⁴ ($E_O^{\text{TS}} = 4.17$ eV).

To further shed light on the direct K–O bonding at TS(K)¹, we have calculated the local density of states (LDOS) projected onto the O atom at TS(K)¹ (Figure 7c). This is illustrated with the LDOS projected onto the K atom from the K/Rh(111) (Figure 7a) and the LDOS projected onto the O atom at the TS^o (Figure 7b). All the LDOSs are calculated by cutting small volumes with a 0.3 Å radius at the center of the K or the O atom. For K adsorption (also see the total charge density difference plot in Figure 1b), Figure 7a shows only one peak at about –14 eV that corresponds to the K 3p state, and the K 4s electrons are hardly found near the K atom, implying a large delocalization of K 4s electrons. Figure 7b examines O bonding at TS^o: The first peak (around –11 eV) contains C 2s electrons delocalized into the O atom. The later quantum states from –9

(54) Mortensen, J. J.; Hammer, B.; Norskov, J. K. *Surf. Sci.* **1998**, *414*, 315.

eV to the Fermi level (E_F) are mainly mixing states between the O 2p and the Rh s, d states. Compared to the O atom at TS^o (Figure 7b), the most striking feature for O at TS(K)¹ (Figure 7c) is the additional peak around -14 eV, which is in a region with strong K 3p character (Figure 7a). This clearly demonstrates the delocalization of K 3p electrons toward the O atom and indicates the nascent K–O bonding at TS(K)¹.

It is worth mentioning some experimental observations that were suggested as evidence for the existence of K–O direct bonding in coadsorbed states. Toomes and King⁷ have observed K–O π resonances for CO and K coadsorption on Co(10 $\bar{1}$ 0), and the coadsorption structure determined also favors such a direct K–O bonding. More importantly, isotopic scrambling phenomena have been observed for many K + CO coadsorption systems. Bonzel²⁶ proposed a direct K–O bonding model to explain such an observation. This mechanism is supported by many other experiments (see discussions in ref 7 by Toomes and King).

4.2. K-Induced Interaction Energy Decrease at the TS.

Table 4 shows that K can also reduce $E_{\text{int}}^{\text{TS}}$. However, the decrease of $E_{\text{int}}^{\text{TS}}$ is not directly related to the distance between K and the TS complex: $E_{\text{int}}^{\text{TS}}$ values in both TS(K)¹ and TS(K)⁴ are quite similar (reduction of 0.17 and 0.16 eV, respectively), although the distances between K and the TS complex in TS(K)¹ and TS(K)⁴ are very different.

As we mentioned before, $E_{\text{int}}^{\text{TS}}$ contains mainly two contributions: (i) the *bonding competition* effect and (ii) the *direct Pauli repulsion* between the C and O atoms. We have used the following approach to further examine if K influences directly the bonding competition between C and O. A *standard bonding competition energy*, defined as E_{int}^0 , for the C + O coadsorption system was calculated as follows:

$$E_{\text{int}}^0 = E_C + E_O - E_{\text{C+O}} \quad (6)$$

where $E_{\text{C+O}}$ is the total chemisorption energy of C + O coadsorption in which the C and O atoms are placed at two neighboring hcp sites in a p(3 \times 3) unit cell (thus they share one surface atom) and the positions of C and O correspond to their individual optimized adsorption positions; E_C (E_O) is the individual chemisorption energy of C (O). In such a structure, the distance between C and O is about 2.7 Å, at which the direct Pauli repulsion is believed to be negligible. Thus, E_{int}^0 measures mainly the bonding competition effect between the C and the O. The calculated E_{int}^0 is 0.38 eV. When K was placed on another hcp hollow site, which is directly adjacent to both C and O (*the C and O were fixed*), $E_{\text{int}}^0(\text{K})$ was calculated to be 0.36 eV. The small difference between E_{int}^0 and $E_{\text{int}}^0(\text{K})$ implies that the K has almost no direct effect on C and O bonding competition if the C and the O were fixed. This is reasonable considering that K–Rh(111) bonding is not covalent (see section 3.1), and the adsorbed K atom has little effect on the d orbital of the adjacent surface atoms. Therefore, K should have little influence on the C–O bonding competition through its effect on the Rh d orbital. This is consistent with the work of Mortensen et al.,⁸ who found that the alkali metal has little effect on the metal d band structure.⁵

Although the surface d states are only slightly affected by K, K can modify the TS structure through the increase of the electron density near the surface (the increase of surface s electrons, see Figure 1b). The change in the TS structure will in turn modify $E_{\text{int}}^{\text{TS}}$. Therefore, the similar $E_{\text{int}}^{\text{TS}}$ reduction at TS(K)¹ and TS(K)⁴ can be understood considering that the structure changes at the TSs are largely mediated by the rather delocalized surface s electrons. In particular, the TS structures

listed in Table 2 show that in K-promoted CO dissociation, both C and O *move away* from the Rh(111) surface at the TSs (C–Rh and O–Rh bond lengths increase), and the C–O distance becomes *longer*. These structural changes lead to (i) a reduction of the bonding competition between the C and the O, since both the C and the O are less strongly bonded with the surface (the covalent bonding of C (O) with metal is weakened), and (ii) reduced Pauli repulsion between C and O, considering that the direct Pauli repulsion is a function of C–O distance.

4.3. Implications of the Direct Bonding Mechanism. It is of interest to compare the results for the K promotion effect presented above with the S poisoning effect in heterogeneous catalysis. In contrast to K adsorption, S adsorption on transition metal surfaces is similar to C and O adsorption, namely, being largely covalent. Specifically, the S 3p orbitals will mix with metal d orbitals, if available. It has been suggested by several groups that the S-modified metal d states become inert, and thus the reactivity is reduced.^{5,55,56} We expect that the basic differences between K and S effects are that (i) K atoms do not significantly interfere with metal d orbitals, but S atoms do,^{5,56} and (ii) K atoms increase the surface s electrons, while S atoms reduce surface s electrons (near the Fermi level).⁵⁵ As a result of strong mixing between S 3p and metal d orbitals, the TS complex of a reaction will be destabilized if the S atom is adjacent to the TS: The reactants–surface bonding will be significantly weakened. This effect is rather short-range, requiring S and the reactants to share surface atoms at the TSs. As to the long-range aspect of the S poisoning effect, Feibelman and Hamann suggested that it is due to the S-induced surface electron depletion near the Fermi level.¹² Therefore, we expect that to determine the S poisoning effect on reactions, like CO dissociation, each term in eq 5 should also be varied, but in the opposite direction to those in the K promotion effect: E_C^{TS} and E_O^{TS} should be reduced, while $E_{\text{int}}^{\text{TS}}$ should be increased.

In contrast to the S poisoning effect, K will directly interact with the reactants, which in most cases stabilize the reactants and promotes reactions. There is an exception: K can poison H₂ dissociation on transition metal surfaces, which is similar to the effect of S.^{9,56} For H₂ dissociation on Pd(100), for example, DFT calculations by Wilke and Cohen⁹ have confirmed the experimental observation: H₂ dissociation is poisoned by K addition, even though K can still stabilize the H atom adsorption at the FS. We may understand this puzzle as follows. Considering the quite small electronegativity of the H atom, the K–H bonding, if it exists, is rather weak compared to K–O bonding. Therefore, the K effect on H₂ dissociation should not be dominated by direct bonding between K and H₂, which was indeed not observed by Wilke and Cohen. However, the adsorbed K atoms can donate their 4s electrons to the surface to form a delocalized electron layer on the surface (see Figure 1b). This will increase the Pauli repulsion between the surface s electrons and the approaching close-shelled H₂, which should pile up the reaction barrier at the *entrance channel*, as pointed by Harris and Andersson.⁴⁶ Such an early TS implies that the K–H direct bonding would not help the H₂ dissociation. Furthermore, it is also implied that the K poisoning effect on H₂ dissociation is rather *long-range*, which has little relationship with the distance between the K and the dissociating H₂. Both features have been indeed identified in the calculated results for H₂ on K-covered Pd(100).⁹

It should be emphasized that for the alkali-promoted CO dissociation the Brønsted–Polanyi relation is not followed. The

(55) Goodman, D. W. *Appl. Surf. Sci.* **1984**, *19*, 1.

(56) Wilke, S.; Scheffler, M. *Phys. Rev. Lett.* **1996**, *76*, 3380.

Brondsted–Polanyi relationship⁵⁷ states that for similar reactions, the reaction barrier change (ΔE_a) is proportional to the reaction energy change (ΔE_r) ($\Delta E_a = \Delta E_r/2$). This means that the addition of K should stabilize the TS to a lesser extent than its effect to the FS. However, our results show that the CO dissociation barrier on Rh(111) can be lowered by as much as 0.51 eV with K coadsorption, while in the FS the maximum stabilization (C, O) in the presence of the K is about 0.27 eV (for the C at nearest-hcp and the O at nearest-fcc). Therefore, the K stabilization effect on the TS is considerably higher than its effect on the FS.

Finally, it is worth discussing the K effect on the reverse reaction of CO dissociation, namely the association reaction, $C + O \rightarrow CO$, on Rh(111). Our calculated barrier for the association reaction is 1.75 eV on clean Rh(111) ($p(3 \times 3)$). In the presence of K, our calculations show a decrease in the association reaction barrier by 0.24 eV if the $TS(K)^1$ is considered. This suggests that K can also promote the association reaction. However, if only $TS(K)^3$ and $TS(K)^4$ are the possible TSs, where no direct K–O bonding exists and the decrease of dissociation barrier is small, then the K would poison the $C + O$ association reaction. The reason for this is that the distances between K and the C–O TS complexes in the $TS(K)^3$ and $TS(K)^4$ are quite long, and thus the TSs are stabilized by the K to a lesser extent compared to the corresponding FSs. Experimentally, the K promotion effect on the $C + O$ reaction on Rh(111) has been indeed observed by Kiss et al.⁵⁸ This strongly suggests the existence of the $TS(K)^1$ or $TS(K)^2$ and indicates in turn the importance of direct K–O bonding in the K promotion effect.

5. Conclusions

Having carried out extensive DFT calculations and one of the most detailed analyses, we now have a deeper understanding of the alkali promotion effect in heterogeneous catalysis. The following conclusions are reached:

1. For K adsorption on Rh(111), K significantly donates

(57) See, e.g.: van Santen, R. A.; Neurock, M. *Catal. Rev. Sci. Eng.* **1995**, 37, 557.

(58) Kiss, J.; Klivenyi, G.; Revesz, K.; Solymosi, F. *Surf. Sci.* **1989**, 223, 551.

electrons (mainly the K 4s electrons) to the metal surface, forming a delocalized electron layer near the surface. For O adsorption, the O–Rh covalent bond is formed through the O $2p_{x(y)}$ and Rh d orbitals, and the charge accumulation is not along the axis through the center of the Rh and the O atoms. There is a charge depletion in the O $2p_z$ orbital and the surface s electrons just beneath the O atom.

2. In the simple coadsorption systems, $K + O/Rh(111)$ and $K + C/Rh(111)$, the nature of the K–adatom (O or C) interaction depends on the adatom (O or C) and, especially, the K–adatom distance. Generally, when K is farther away from the adatom (4–5 Å), the interaction is of an electrostatic origin, and the K-induced adsorption energy change is rather small, within 0.05 eV. When K is at closer configurations (K–adatom distance being 3–4 Å), direct bonding between the K and the adatom occurs, and the K-induced adsorption energy change is up to 0.1–0.2 eV.

3. K promotion in CO dissociation on Rh(111) strongly depends on the distance between K and the dissociating CO. The CO–K distance is <3 Å, and the reaction barrier is almost half that for CO dissociation on clean Rh(111). For configurations when K is >4 Å away from the dissociating CO, the induced barrier change is relatively small. Two important reasons are found to account for the K promotion effect:

- (i) If the distance between K and the dissociating CO is short (2–3 Å), the direct K–O bonding is observed, which greatly stabilizes O at the TS and thus reduces the dissociation barrier. *This is the main physical origin of K promotion in CO dissociation.* On the other hand, when the distance is long, only the electrostatic interaction exists, which only slightly stabilizes the reactant at the TS.

- (ii) Due to the delocalized surface s-like electrons donated by the K, the lengths between the TS complex and the Rh atoms involved are increased, leading to a reduction of the interaction energy between the C and the O. This decrease in the interaction energy further reduces the dissociation barrier.

Acknowledgment. The supercomputing center for Ireland is acknowledged for computer time.

JA011446Y